CODEN STJSAO
ZX470/1452

ISSN 0562-1887
UDK 629.735.036.7:681.515.8

Control of Electro-Mechanical Actuator for Aerospace Applications

Muhammad Ashraf KHAN, Ivana TODIĆ, Marko MILOŠ, Zoran STEFANOVIĆ* and *Đorđe BLAGOJEVIĆ

Mašinski fakultet, Univerziteta u Beogradu,
(Faculty of Mechanical Engineering,
University of Belgrade),
Kraljice Marije 16, 11120 Beograd,
Republic of Serbia

mmilos@mas.bg.ac.rs

Keywords
Brushless DC Motor
Electro-Mechanical Actuator
PID controller
Planetary Roller Screw
Sensor
Thrust Vector Control

Ključne riječi
Elektro-mehanički pokretač
Istosmjerni motor bez četkice
Osjetnik
PID kontroler
Planetarni prijenosni sistem
Upravljanje vektorom potiska

Received (primljeno): 2009-11-29
Accepted (prihvaćeno): 2010-05-12

Original scientific paper

The paper mainly focuses two major areas of electromechanical actuator system composed of power screw, spur gear train and Brushless DC Servo Motor. First it describes control of electromechanical actuator system with three level of current controller which is composed of power amplifier, DSP module and interfacing circuitry. The non-linear model of the three level controllers developed in SIMULINK environment is presented. A second point which was included in this study is the comparison of two control strategies i.e. three level controller and PWM current controller. The main outcomes of the study is that three level controller is simple in construction and much more stable. This is much suitable for higher reduction systems, short missions and low power density actuators; however it has few limitation that make it unsuitable for applications such as high power density, long missions and direct drive system.

Upravljanje elektro-mehaničkim pokretačem za primjene u zrakoplovnim sustavima

Izvornoznanstveni članak

Ovaj se rad u osnovi fokusira na dvjema glavnim područjima vezanih za elektro mehanički pokretački sustav, koji je sačinjen od pogonskog vijka, prijenosnog sistema i istosmjernog motora bez četkica. Prvo je opisano upravljanje elektro mehaničkim pokretačkim sustavom pomoću kontrolera sa tri nivoa struje, koji je sačinjen od DSP procesorskog modula i elektronskog kola sa pojačivačem. Prikazan je i nelinearan model kontrolera sa tri nivoa struje koji je razvijen u SIMULINK okruženju. U radu je također prikazana usporedba dvaju tipova kontrole: kontroler sa tri nivoa struje i PWM strujni kontroler. Glavni zaključci na osnovi dobijenih rezultata su da je kontroler sa tri nivoa struje jednostavniji za izradu i mnogo stabilniji. Njegova primjena posebno je pogodna u sustavima sa velikom redukcijom, u kratkotrajnim misijama i sustavima s manjom izlaznom snagom; ipak ukazano je i na nekoliko nedostataka: nije preporučljivo koristiti ga pri većim snagama i u dužem vremenskom razdoblju uslijed većih toplotnih gubitaka.

1. Introduction

The use of an electromechanical actuation system is becoming increasingly popular in the aerospace community for a variety of reasons that include maintainability, reduced number of parts, rapid production and reduced weight and costs. Recent studies have shown that hydraulic actuation systems cost the space program many valuable hours for tests, maintenance and repairs [2, 5, 13-14]. During a typical turnaround cycle for a space shuttle orbiter and its integrated systems, many maintenance personnel inspect the entire vehicle, repairing hydraulic leaks and examining lines, while at the same time qualifying each hydraulic unit for its next flight. Qualification alone necessitates extensive hours, or about 10 percent of the total inspection time. Estimates submit that fully electric orbiters could possibly be readied for flight ten days earlier than hydraulic ones. These problems affecting mission readiness have prompted investigations by NASA into alternate actuation systems for use in existing space applications, as well as new programs soliciting heavy lift TVC technology. Some reservations of implementing electric TVC systems into these very new programs overshadow the fact that EMAs have been in service for more than thirty years. A good example of an early EMA technology application is the Redstone Missile in the 1950's. In this system, an electrical chain drive actuated air fins for aerodynamic steering. As early as 1972, NASA engineers expressed concern over the space shuttle's hydraulic system due to difficult maintainability and some minor inefficiency. In the last few years, many advances in the fields of power electronics and motor technology have renewed interest in the use of EMAs for both low and high power actuation

Symbols/Oznake

θ - fin angle, rad
- kut otklona krila

θ_r - rotor angle, rad
- kut rotora

θ_{max} - maximum dedlection of fin, rad
- maksimalni dopušten otklon krila

ω_r - angular velocity of rotor, rad/s
- kutna brzina rotora

λ - amplitude of the flux induced by the permanent magnets of the rotor in the stator phases, which can be calculated from the torque constant (which is given by motor manufacturer)
- amplituda toka induciranog između stalnog magneta rotora i faza statora, koji se može sračunati na osnovi momentne konstante (koju daje proizvođač)

$\Phi'_a, \Phi'_b, \Phi'_c$ - a, b and c phase electromotive forces here

$$\Phi' = -\frac{d\Phi}{dt}$$ (Faraday`s law)

- elektromotorna sila po fazama a, b i c gdje je

$$\Phi' = -\frac{d\Phi}{dt}$$ (Faradejev zakon)

η - efficiency
- stupanj korisnosti

F - viscous friction coefficient, Nms
- koeficijent viskoznog trenja

F_g - viscous friction coefficient in gearbox, Nms
- koeficijent viskoznog trenja u reduktoru

G - gearbox ratio
- prijenosni odnos reduktora

$i_a, i_b, i_c,$ - a, b and c phase currents
- struja po fazama a, b i c

J - total inertia, inertia of motor and its load, kg·m^2
- ukupni moment inercije na strani motora

K_a - torque constant, Nm/A
- momentna konstanta

K_f - static friction coefficient
- koeficijent statičkog trenja

K_{gf} - coulomb (static) friction coefficient
- koeficijent statičkog trenja u reduktoru

L_A - inductance in phase A, H
- induktivnost faze A

p - number of pole pairs
- broj pari polova

p_t - thread step, mm
- pužni korak

R_A - resistance in phase A, Ω
- otpornost u fazi A

T_m - load torque, Nm
- izlazni moment

T_e - generated electromagnetic torque, Nm
- generiran elektromagnetni moment

T_{amax} - maximum load, Nm
- maksimalno opterećenje

T_{gf} - coulomb (static) friction torque, Nm
- moment uslijed statičkog trenja

T_{gv} - viscous friction torque, Nm
- moment uslijed viskoznog trenja

in space applications. In 1987, the Control Mechanisms and Propellant Delivery Branch at MSFC designed and tested an electromechanical propellant valve actuator applicable to the space shuttle main engine. It performed as well as, and in some areas, better than its hydraulic counterpart. Conventional centralized hydraulic systems used in today's launch vehicles perform well but are an operational nightmare. The cost to maintain and operate these systems is prohibitive and contributes to today's excessive launch costs. In a study conducted by NASA-Kennedy Space Center (McCleskey and Rushing, 1992), it was shown that a cost savings of $3M per flight could be realized by replacing the hydraulic-powered Solid Rocket Booster Thrust Vector Control (TVC) actuator system with an electric one. Studies on other vehicles have shown similar savings and operational advantages to replacing hydraulics with EMA systems. These advantages include: increased reliability, improved safety through the elimination of high pressure and hazardous fluids, reduction in check-out time and increased ability to launch on demand. Likewise, studies on commercial aircraft for NASA'S Power by Wire program have shown significant benefits to replacing the pneumatic and hydraulic systems with an all-electric secondary power system, including EMAs for the control surfaces (Murray, 1992 and Renz, 1992).

Flight validation of the experimental electromechanical actuators was conducted on Dryden's Systems Research Aircraft (SRA), a highly modified F-18 Hornet, under the Electrically Powered Actuation Design (EPAD) program. EPAD engineers estimate that adopting electrically-driven actuators for all flight control surfaces could lead to a five percent to nine percent fuel savings on an all-electric passenger plane and a 30 percent to 50 percent reduction in ground equipment. Military tactical aircraft could achieve a 600 to 1,000 pound reduction in take-off weight, and a 14 percent reduction in the area that is vulnerable to such threats as small arms fire. David

Dawson, AFRL Air Vehicles Directorate EPAD program manager, called EPAD a major milestone on the road to an all-electric airplane. "The experience gained by flying power-by-wire actuators on NASA's Systems Research F-18 provides confidence for the next step in power-by-wire development: flight demonstration of a more- electric aircraft," Dawson said. "EPAD is on the critical path toward realizing the AFRL's More Electric Aircraft initiative." Theses are the few facts, which attract military and commercial aerospace community to work on electromechanical actuator systems. Evidence of the shift towards EMA technology can be found in the Power by Wire in the U.S air force and the commitment of NASA to use all electric actuation on future spacecrafts. X-33 Advanced technology demonstrator is one such spacecraft.

Modeling and simulation is an important step in design and development of actuator systems. This paper presents a nonlinear model of linear electromechanical actuator systems with three step of current control to the actuator system. To regulate the power that flows from power supply to the actuator can be made either by regulating current or voltage. Historically it was done mostly by voltage control, but over the last few decades the technology that preferred is to control the current. The current can be regulated in many way i.e. linear control, pulse width modulated control and the three level current control. Every mechanism of current control has its own pros and cones. The paper will present all of them in detail in the coming sections. Also the reasons for adopting three level current control strategies will be analyzed in comparisons with pulse width modulation techniques for some example cases.

2. DC motor controller, basic principle

Usually pulse-width modulation circuit is used for control of DC brushless motor. The pulse-width modulation circuit outputs pulse-width modulation signals according to the polarity and intensity of input signals [3, 7, 9, 12]. The bridge power driving circuit applies different voltages to the two ends of the motor according to the input signal to rotate the motor shaft in different directions, shown on Figure1.

2.1. "Constant" current controller

In this case a different solution for control of DC brushless motor is used. The motor is controlled with three levels of 'constant' current: zero current, nominal

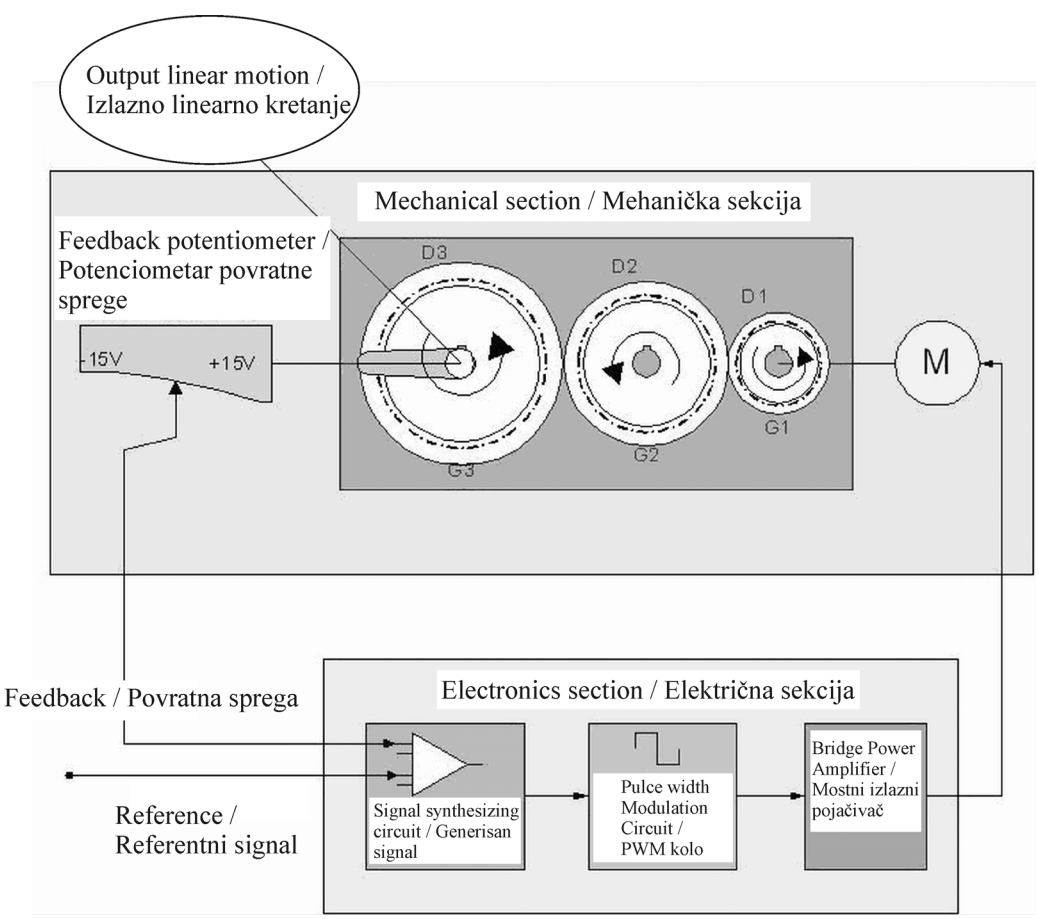

Figure 1. Schematic of linear mechanical actuator system control by PWM principle

Slika 1. Shema linearnog elektro mehaničkog pokretačkog sistema sa PWM kontrolom

and high current, shown on Figure 2. This solution is simpler but it has some limitation on high power system, which can be seen later on in the text.

phase winding of the stator. Relative position of the rotor is signaled by three hall sensors, which are mounted 120 deg around the internal armature of the motor. They are

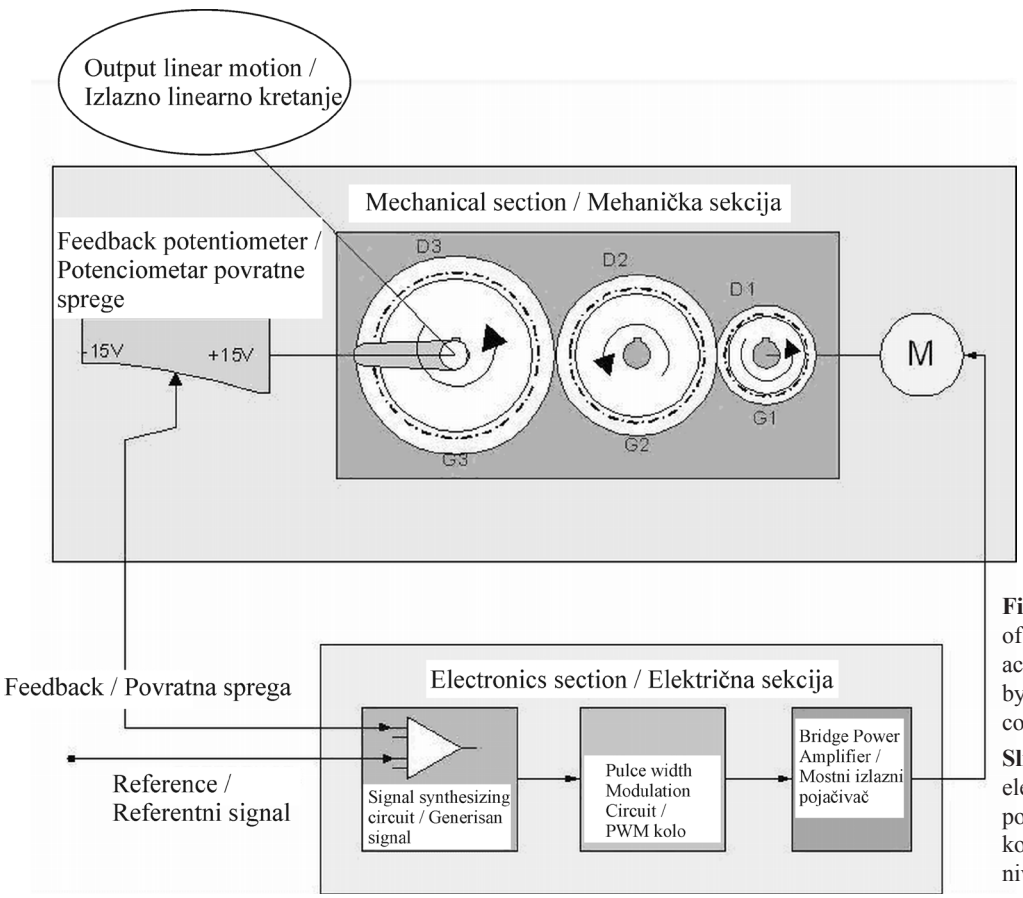

Figure 2. Schematic of linear mechanical actuator system control by constant current controller

Slika 2. Shema linearnog elektro mehaničkog pokretačkog sistema sa kontrolerom na bazi tri nivoa struje

Motor controller consists of the following parts:

- Power Amplifier
- DSP (Digital Signal Processor) Module
- Interface circuits-Motor Multiplexer

The Power Amplifier is used to produce phases switching at appropriate moments (similar to the function of the commutator on DC brushed motor). A second function of the amplifier is to supply the motor-phases with almost constant current. Using a constant current source allows more robust handling of the motor and protection from overheating on the one hand, and allowing proposed control in the loop on the other hand.

The amplifier is made to be connected to the battery supply. Concerning that single battery supply and the need for positive and negative current for phase driving, it is proposed to use full-bridge 3-phase driver, which consists of three separate half-bridge transistors driver. If the brushless DC motor (BLDC) has no neutral connection, the phase windings are connected in a triangle (delta) and at each moment the current is "passing" only through one positioned in such way that the controller can distinguish on which connecting point of the motor supply voltage has to be fed, and on which battery ground it is supplied. In such a way, it is possible to deliver to the motor positive or negative current to each phase winding.

In order to limit the current during the driving phase, measuring of the voltage through the sensing resistor is done, and when the current passing through the phase winding electronic sensing circuitry break connection of the phase winding to the supply DC battery is attained. After that moment the phase current starts to lessen. Current monitoring circuits (with hysteresis) activate the proper transistors to enlarge the current again. Such way of controlling the current can produce a switching signal with very high frequency. In order to have greater influence on the switching signal frequency, control is designed that OFF time of the switching transistors is constant and controlled by 'one-shot' circuitry.

Depending on calculated current, the amplifier can supply the phase with three values of current; zero current, nominal and high current, which is about 50 % larger

than nominal one, depending on system requirements. The nominal current corresponds to the motors nominal stall current. This level of current should be enough to hold the rotor (over gearbox) under maximal load. But in order to allow dynamic movements of the rotor, the current has to be enlarged. When the actuator reaches the desired position (desired angle), and if no other movements are required, the current can be lowered to the nominal value. To overcome larger moments (consisting of the load and dynamic loading, which mainly "consist of" rotor moment of inertia) more current has to be fed to the motor windings, but not for a long time in order to prevent overheating of the motor itself.

Here it has to be emphasized that when the motor reaches the angular speed which is near maximum for the applied power supply - back electromotive force (BEMF) that is inducted because of rotor rotation can reduce the desired current and the driving circuit (for gate diver) can fail to drive the "upper" transistor. This can lead to the motor in an off state (because the driver of the "upper" – or "high side" transistor needs some switching pulse to load the "high side" gate driver. To prevent such situation small self-oscillating circuitry starts to oscillate whenever voltage between Vb and Vs is less than 10V, charging the capacitor to about 10V, which is enough for normal operation of the "high side" FET driver.

A sensing resistor controls the value of the desired current and then its value is compared to the desired voltage. If from DSP side (algorithm) larger current than nominal is required, the transistor changes to 'switch off' state, which would raise the referent voltage by about 50 %. The current "limiting" would be risen by 50 %.

Control of the appropriate phase switching is done by the DSP in coordination with hall sensors output. DSP sends three control signals, which are 'resampled' in order to lower the possibility for glitches to occur. The outputs are connected to logic circuits that generate the control signals for the controlling transistors in the output stage.

The presented amplifier has a built-in option for control based on direction control of the rotor rotation only (CW = "clock wise" or CCW ="contra clock wise"), but real switching between phases is controlled directly by the hall sensors. Of course, DSP can allow starting its rotation, or can "freeze" the desired state of the hall sensors (if it is decided that rotor has to stay at reached position but with the current energized one phase winding).

3. Stability and dynamics characteristic of system

It is very difficult to give an exact function of the actuator system, because this system is not a linear system. But here some basic stability and dynamics characteristics of the actuator system will be considered.

First, the most important thing that should be remembered is that this controller works with current (not voltage), and that there are three conditions for controlling the current: zero current, nominal current and high current. Here it is assumed that a motor model can be presented like the equivalent electric circuit, as on Figure 3. [4, 8, 10-11].

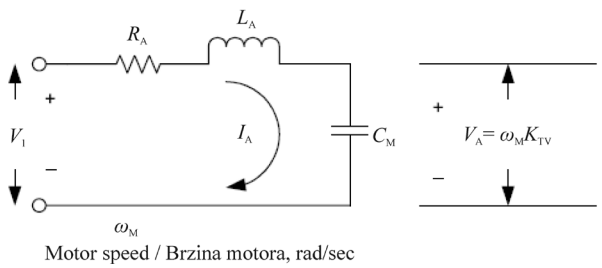

Figure 3. Schematic of motor model presented by equivalent electric circuit

Slika 3. Prikaz modela motora ekvivalentnim strujnim kolom

Where

$$C_M = \frac{J}{K_a^{\,2}}. \tag{1}$$

Now the transfer function for the motor is:

$$\theta = \frac{1}{Gs}\omega,$$

$$\omega K_v = V = \frac{I}{Cs},$$

$$\Rightarrow \frac{\omega}{I} = \frac{1}{K_a Cs} = \frac{1}{K_a \frac{J}{K_a^{\,2}} s} = \frac{K_a}{Js}, \tag{2}$$

$$\Rightarrow H_M(s) = \frac{\theta}{I} = \frac{K_a}{JGs^2}.$$

Also the transfers function for the PID regulator:

$$H_{PID}(s) = A_o \frac{K_i + K_p s + K_d s^2}{s}. \tag{3}$$

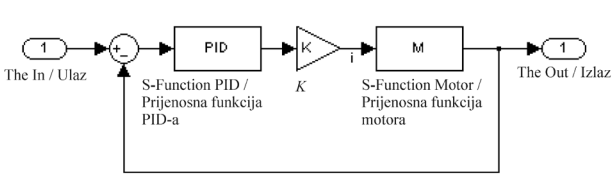

Figure 4. Block diagram of DC brushless motor with PID regulator

Slika 4. Blok dijagram istosmjernog motora bez četkica sa PID regulatorom

Now the transfer function for the actuator system, based on the scheme on Figure 4 can be written:

$$H(s)=\frac{KH_{\mathrm{PID}}(s)H_{\mathrm{M}}(s)}{1+KH_{\mathrm{PID}}(s)H_{\mathrm{M}}(s)}.$$

Where

K - is gain which presents limiting of current in two states, and only variable

$$H(s)=\frac{\frac{K_{\mathrm{d}}}{K_{\mathrm{i}}}s^2+\frac{K_{\mathrm{p}}}{K_{\mathrm{i}}}s+1}{\frac{GJ}{K_{\mathrm{i}}A_{\mathrm{o}}K_{\mathrm{o}}K}s^3+\frac{K_{\mathrm{d}}}{K_{\mathrm{i}}}s^2+\frac{K_{\mathrm{p}}}{K_{\mathrm{i}}}s+1}. \quad (4)$$

Because of the high increment for small errors and on the other side decrement on higher errors it will be assumed that $K \in [0.1, \ldots, 1]$ to see how K affects dynamics and stability of system.

First it will be shown how an increase of K will have an effect on higher errors, where $K \in [0.1, \ldots, 1]$. Results are shown in Figure 5.

Effects of increase of K on small errors, where $K \in [1, \ldots, 10]$, are shown in Figure 6.

From this consideration it can be concluded that stable systems have much better dynamic on small errors, which means smaller overshoot and settling time. Also we can conclude stability for all value of K.

4. Description of the mathematical modeling

A simple mathematical relationship between the shaft angular velocity and voltage input to the DC brushless motor might be calculated from physical laws.

First the mechanical part of DC brushless motor can be described. From Newton's law of motion, the following relationship may be obtained:

$$J\frac{d\omega_{\mathrm{r}}}{dt}=T_{\mathrm{e}}-T_{\mathrm{m}}-F\omega_{\mathrm{r}}. \quad (5)$$

The angular position may be obtained from an integration of the angular velocity.

$$\theta_{\mathrm{r}}=\int \omega_{\mathrm{r}}\mathrm{d}t. \quad (6)$$

The next thing that should be explained is the electrical part of DC brushless motor and relationship between currents, voltage, and beck electromotive force and rotor velocity. Next equations are expressed in the phase reference frame (ABC frame).

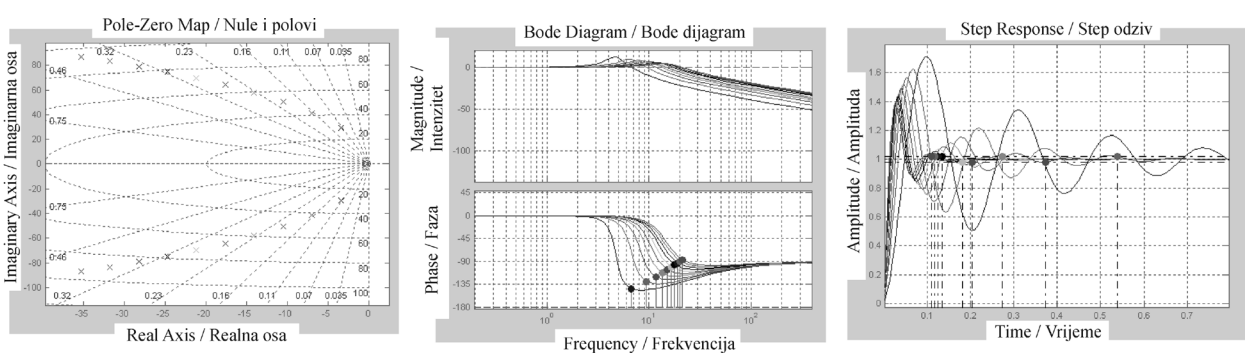

Figure 5. Stability and dynamic characteristic of system for high errors

Slika 5. Stabilnost i dinamičke osobine sistema pri većim ulaznim greškama

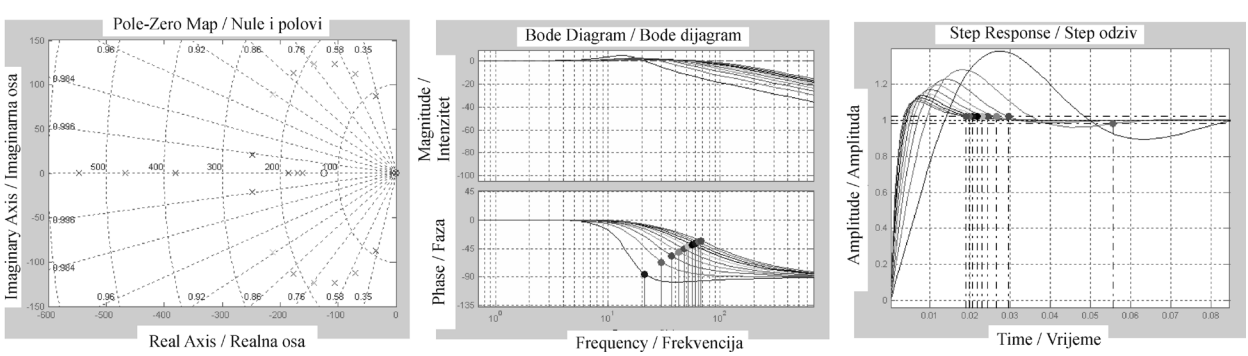

Figure 6. Stability and dynamic characteristic of system for small errors

Slika 6. Stabilnost i dinamičke osobine sistema pri manjim ulaznim greškama

$$L_s \frac{d}{dt} i_a + R_s i_a = \frac{1}{3}\left[2v_{ab} + v_{bc} + \lambda p \omega_r \left(-2\Phi'_a + \Phi'_b + \Phi'_c\right)\right]$$
$$L_s \frac{d}{dt} i_b + R_s i_b = \frac{1}{3}\left[-v_{ab} + v_{bc} + \lambda p \omega_r \left(\Phi'_a - 2\Phi'_b + \Phi'_c\right)\right]$$
$$\frac{d}{dt} i_c = -\left(\frac{d}{dt} i_a + \frac{d}{dt} i_b\right). \quad (7)$$

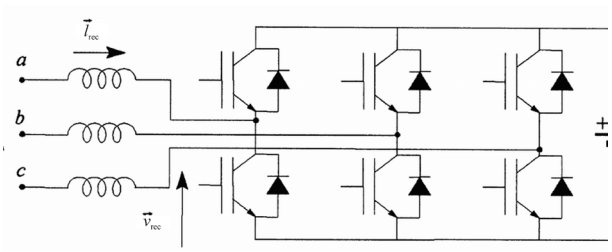

Figure 7. Schematic of DC brushless motor

Slika 7. Shematski prikaz istosmernog motora bez četkica

Generated electromagnetic torque is given by

$$T_e = p\lambda\left(\Phi'_a i_a + \Phi'_b i_b + \Phi'_c i_c\right). \quad (8)$$

Where [1, 6]

- Sinusoidal flux distribution

$$\lambda = K_a \frac{\sqrt{2}}{3p},$$

- Trapezoidal flux distribution

$$\lambda = \frac{K_a}{2p}.$$

Because in this case is trapezoidal flux distribution, it can be used next basic equations for calculating electromotive force.

$$\Phi'_a = \frac{C_a}{\text{trap}},$$
$$C_a = f\left(\cos\theta_e\right),$$
$$f\left(\cos\theta_e\right) = \begin{cases} \cos\theta_e; & -\text{trap} \le \cos\theta_e \le \text{trap} \\ \text{sgn}\left(\cos\theta_e\right)\text{trap}; & \left|\cos\theta_e\right| > \text{trap} \end{cases},$$
$$\text{trap} = \sin\frac{\pi\left(1 - \frac{flat}{180}\right)}{2}.$$

Where

flat - Back EMF flat area [degrees], we can use sinusoidal flux distribution if we set flat = 0

$\theta_e = p\theta_r$ - Electrical angle

$$\Phi'_b = \frac{C_b}{\text{trap}},$$
$$C_b = f\left[\cos\left(\theta_e - \frac{2\pi}{3}\right)\right],$$
$$\Phi'_c = \frac{C_c}{\text{trap}},$$
$$C_c = f\left[\cos\left(\theta_e + \frac{2\pi}{3}\right)\right].$$

Load torque is calculated like sum of coulomb friction of motor, load torque and coulomb and viscous friction in gearbox.

$$T_m = T_f + T_A + T_{gf} + T_{gv}. \quad (9)$$

Coulomb friction of motor may be obtained from next relationship

$$T_f = K_f \text{sgn}\left(\omega_r\right) \quad (10)$$

Before we obtain load torque we should express the gearbox function, because load torque is the function of fin angle and we have, for now, motor angle.

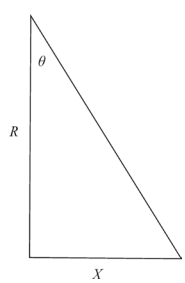

$$\tan\theta = \frac{x}{R} = \frac{p_t \frac{\theta_r}{2\pi}}{R} = \frac{p\theta_r}{2\pi R},$$
$$\theta = \arctan\left(\frac{p\theta_r}{2\pi R}\right).$$

Load torque is the function of deflection.

$$T_A = \frac{\sin\theta}{\sin\left(\theta_{max}\right)} \frac{T_{amax}}{G} \frac{1}{\eta} \qquad \omega_r\theta > 0,$$
$$T_A = \frac{\sin\theta}{\sin\left(\theta_{max}\right)} \frac{T_{amax}}{G} \left(2 - \frac{1}{\eta}\right) \qquad \omega_r\theta < 0. \quad (11)$$

In this model friction in gearbox is also simulated, like sum of Coulomb (static) friction and viscous friction.

$$T_{gf} = \frac{K_{gf}}{G} \text{sgn}\left(\omega_r\right),$$
$$T_{gv} = \omega_r \frac{F_g}{G}. \quad (12)$$

5. Simulating results

A simulation for linear electromechanical actuator for TVC is made in SIMULINK. In a simulation standard SIMULINK blocks and SimPowerSystems blocks are used. More about mathematical modeling of linear electromechanical actuator is given in appendix.

The different types of control are tested separately with simulator; Control with three level of constant current and control with continual current limited on high current (similar PWM), with different PID constant and similar dynamics. Real requirements for three different actuator systems are simulated. The basic difference in these actuator systems lies in their power requirements.

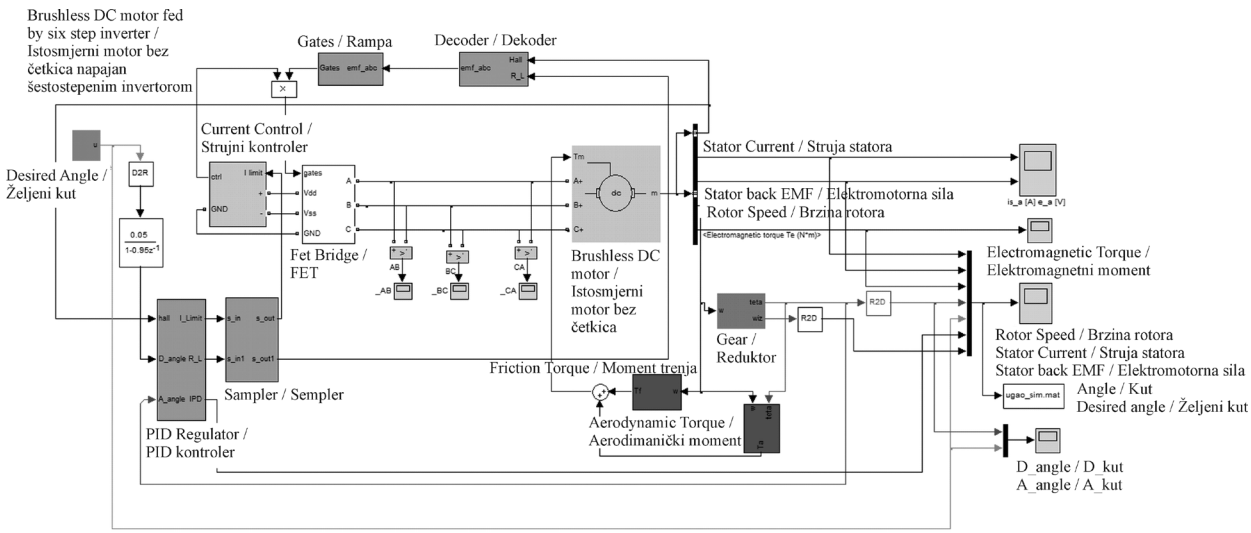

Figure 8. SIMULINK scheme of linear electro-mechanical actuator system

Slika 8. Simulink shema linearnog elektro mehaničkog pokretačkog sistema

5.1. DC brushless motor Moog Bn28-44af

Nominal power is 289 W

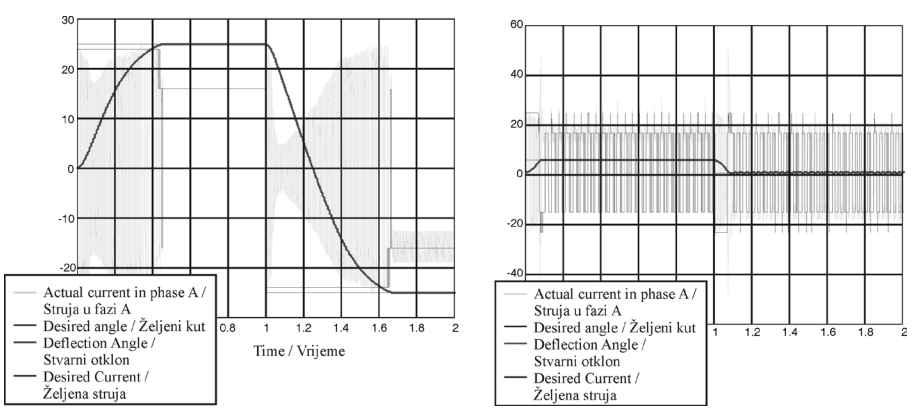

Figure 9. Simulations with constant current controller

Slika 9. Simulacije kontrolera sa konstantnom strujom

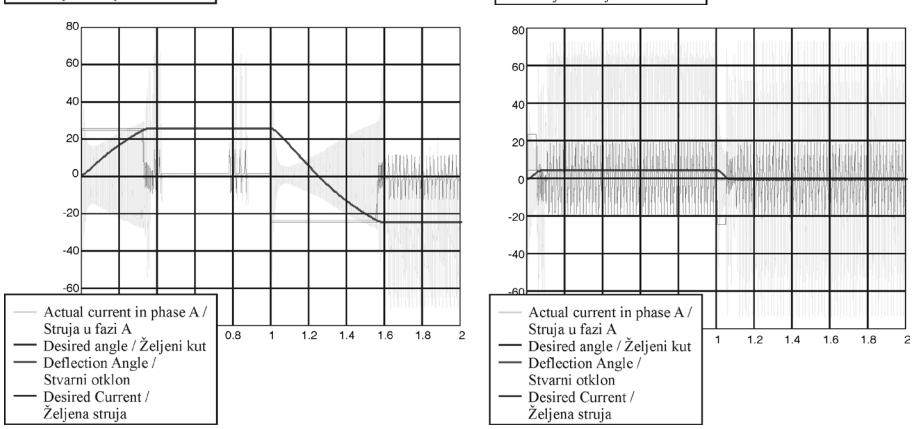

Figure 10. Simulations with PWM controller

Slika 10. Simulacija sa PWM kontrolerom

5.2. DC brushless motor Kollmorgen b-204-c

Nominal power is 2.8kW

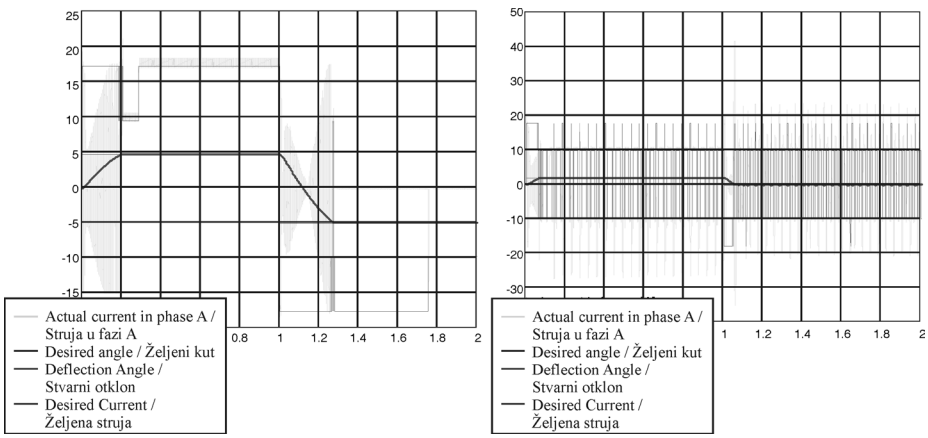

Figure 11. Simulations with constant current controller

Slika 11. Simulacije kontrolera sa konstantnom strujom

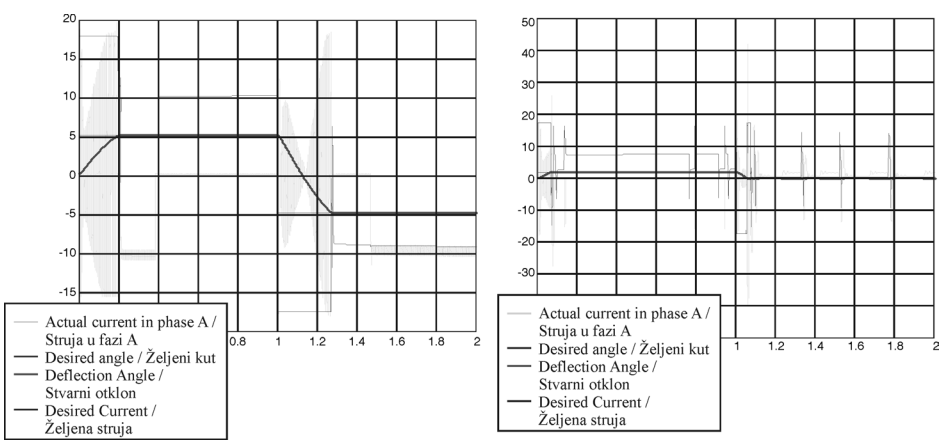

Figure 12. Simulations with PWM controller

Slika 12. Simulacija sa PWM kontrolerom

5.3. DC brushless motor Kollmorgen b-404-c

Nominal power is 5.4kW

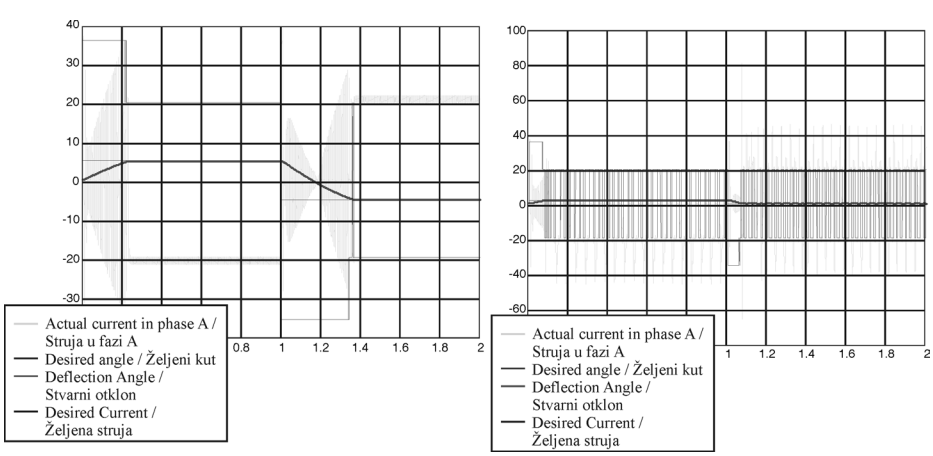

Figure 13. Simulations with constant current controller

Slika 13. Simulacije kontrolera sa konstantnom strujom

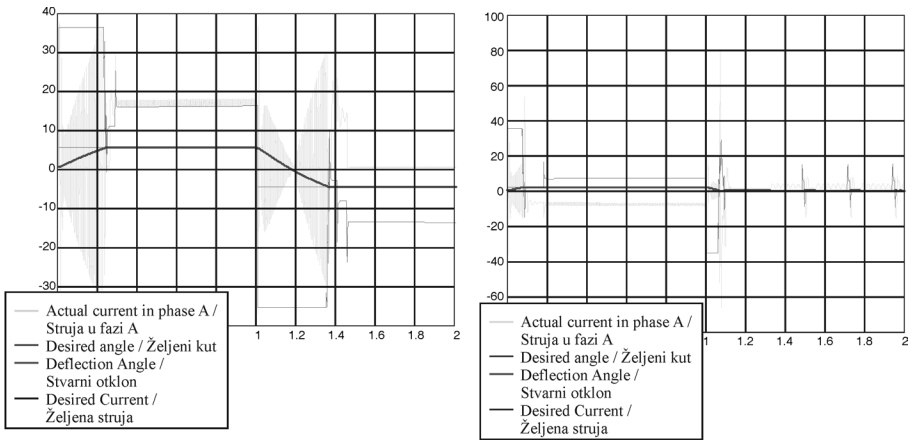

Figure 14. Simulations with PWM controller

Slika 14. Simulacija sa PWM kontrolerom

6. Conclusions

Selection and implementation of any strategy depends on many factors i.e. state variables, precisions, construction, availability of hardware, reliability index mission time, stability and available manpower skills. The strategies were adopted having in mind the mentioned reasons. Following main conclusions can be extracted from the presented work.

- Control with three levels of constant current is the simpler construction.
- This type of control is very stable.
- The method was adopted due to hands on experience on constant current on other system in end use and unavailability of PWM module in the used DSP.
- The system works most of the time at nominal current, which is about 15 Amperes and thus causing more heating; consequently it demands either for special supper conductor heat sink materials or high surface area heat sink.
- The system generates more noise for lower level of errors; this suggests use of higher gear reduction i.e. the noise on output shaft of actuator is lowered by amount of gear reduction; however this will not be the case if the control strategy is used for direct drive system.
- Higher level of precision can be achieved with this strategy by using a feedback sensor; however it suggests high frequency switching (up to 40 Hz) between the current levels as currently it works on about 10 Hz. This will reduce noise at output shaft and precision can be achieved even with lower gears reduction.
- The method adopted is a good solution for short time missions, as for longer mission the power amplifier strain due to high currents flow will reduce components operation time and life.
- The constant current control strategy is a good solution for low power application, however higher current switching between three levels can be problematic and produces more power losses; especially on smaller error signal furthermore this can cause system heating.
- Finally the three levels constant current control is comparable with PWM current control technique in system reliability, construction, ease in implementation, cost in low power applications. However the higher power application will be at the cost of efficiency and system heating. Consequently this encourages PWM current control strategy in high power regime.

Acknowledgements

The authors good like to acknowledge Indjin Ivica M.Sc. E.E. for great assistance during our works on this paper.

REFERENCES

[1] CHIASSON, J.: *Modeling and High-Performance Control of Electric Machines*, IEEE Press Series on Power Engineering, 2005.

[2] COWAN, J.R. and MYERS, W.N.: *Design of High Power Electromechanical Actuator for Thrust Vector Control*, AIAA 91-1849, 1991.

[3] DZUNG, P.Q. and PHUONG, L.M.: *A Modified Space Vector PWM Algorithm for Low-Cost Inverter Control*, International Symposium on Electrical&Electronic Engineering, 2007.

[4] FAN, L.S.; TRIPATHI, A. and KHAMBADKONE, A.M.: *Performance Analysis of Space Vector Modulation*, National University of Singapore, 2003.

[5] GRENIER, D.; DESSAINT, L.A.; AKHRIF, O.; BONNASSIEUX, Y. and LE PIOUFLE, B.: *Experimental Nonlinear Torque Control of a Permanent-Magnet Synchronous Motor Using Saliency*, IEEE TRANSACTIONS ON AUTOMATIC CONTROL, Vol.40, No.5, 1995.

[6] HANSELLMAN, D.C. *Brushless Permanent Magnet Motor Design*, McGraw-Hill, 1994.

[7] KWASINSKI, A.; KREIN, P.T. and CHAPMAN, P.L.: *Time Domain Comparison of Pulse-Width Modulation Schemes*, IEEE TRANSACTIONS ON AUTOMATIC CONTROL, Vol.1, No.3, 2003.

[8] MCCLURE, M.: *A Simplified Approach to dc Motor Modeling for Dynamic Stability Analysis*, Application Report SLUA076-July 2000.

[9] OLESCHUK, V.; BLAABJERG, F. and BOSE, B.K.: *One-Stage and Two-Stage of High Performance Synchronous PMW with Smooth Pulse-Ratio Changing*, IEEE, 2002.

[10] SCHINSTOCK, D.E. and HASKEW, T.A.: *Identification of Continuous-Time, Linear, and Nonlinear Models of an Electromechanical Actuato*r, JOURNAL OF PROPULSION AND POWER, Vol.13, No.5, 1997.

[11] SCHINSTOCK, D.E.; SCOTT, D.A. and HASKEW, T.A.: *Modeling and Estimation for Electromechanical Thrust Vector Control of Rocket Engines*, JOURNAL OF PROPULSION AND POWER, Vol.14, No.4, 1998.

[12] TROUNCE, J.C.; ROUND, S.D. and DUKE, R.M.: *Evaluation of Direct Torque Control using Space Vector Modulation for Electric Vehicle Applications*, University of Canterbury, New Zeland, 2001.

[13] WEIR, R.A. and COWAN, J.R.: *Development and Test of Electromechanical Actuators for Thrust Vector Control*, AIAA 93-2458, 1993.

[14] ZRIBI, M. and CHIASSON, J.: *Position Control of a PM Stepper Motor by Exact Linearization*, IEEE TRANSACTIONS ON AUTOMATIC CONTROL, Vol.36, No.5, 1991.